DE-NOISING OF ULTRASOUND IMAGES FROM CARDIAC CYCLE USING COMPLEX WAVELET TRANSFORM WITH DUAL TREE

BIBICU DORIN [1,2*], MODOVANU SIMONA [1,3], MORARU LUMINITA[1]

[1]*Physics Department, Dunarea de Jos University of Galati, 47 Domneasca St.,800008 Galati, Romania*

[2]*High School Dunarea, Galati, Romania*

[3]*High School Dumitru Motoc, Galati, Romania*

Abstract: The noise is unwanted information which damages the quality of the ultrasound images. For a high quality ultrasound image the noise should be eliminated. The experimental ultrasound image set contains two images of different phases of cardiac cycle. The quality of the obtained result was assessed using the parameters: SNR (signal noise ratio), PSNR (peak signal to noise ratio), MSE (mean error) and MAE (mean absolute error). The results were compared with those obtained by applying a median filter. The conclusion is that the de-noising of ultrasound images with CWT-DT is more efficient than the median filtering method.

Keywords: complex wavelet transform, image quality parameters, de-noising echocardiography images

1. INTRODUCTION

Ultrasounds are used to exploit and to characterize the abnormalities of myocardial structure in echocardiography. The starting point of this study was the observation that removing noise is the necessary pre-processing step of any further processing operation as texture analysis, segmentation, shape identification classification and object recognition. Noise into image appears as random granulation that is particularly visible in uniform areas. The electronic components of the digital devices can generate electrical parasite signals during the acquisition and transmission processes. These parasite signals are superposed over the real image. The commonly noise in an image are salt and pepper or Gaussian noise. This noise consists of random white and black pixels. Cardiac cycle includes all the events related to the blood flow through the heart during a cardiac systole and diastole. Wavelet transform is an important tool in study of 2D images. Wavelet transform has also been successfully used in images de-noise [1-4] and edge detection [5].

In this study, two 2D ultrasound images of different phases of the cardiac cycle were analyzed. Thus, the healthy heart was investigated as a model for the establishment of valuable method to correctly and effective de-noising process. We predict that progress achieved for healthy heart can then be transferred to other cardiac abnormality. To accomplish our task the complex wavelet transform with dual tree is used. An optimal threshold for de-noising operation of the echocardiography has been chosen. The present paper is organized as follows: section 1 is an introduction in our study, in section 2 we present the theoretical methods of the complex wavelet transform

* Corresponding author, email: Dorin.Bibicu@ugal.ro

with dual tree [6] and the formalism used to calculate the SNR, PSNR, MSE, MAE parameters [7-8], the section 3 describes the experimental methods, provides the results and discussions. Finally, the concluding remarks are presented.

2. METHODS

2.1 The complex wavelet transform with dual tree

A wavelet is a component of a signal which was divided into time-frequency components.
A wavelet function [9] satisfies the following requirements:

$$\begin{aligned} &1.\int_{-\infty}^{\infty}\Psi(t)dt=0 \\ &2.\|\Psi\|=1 \end{aligned} \tag{1}$$

The mother wavelet is scaled by a factor s and translated by a factor u in order to obtain a time-frequency family [9]:

$$\Psi_{u,s}=\frac{1}{\sqrt{s}}\Psi\left(\frac{t-u}{s}\right) \tag{2}$$

The wavelet transform applied to a function f, scaled by s and translated by u [9], is:

$$W\ f(u,s)=\int_{-\infty}^{\infty}f(t)\frac{1}{\sqrt{s}}\Psi^{*}\left(\frac{t-u}{s}\right)dt \tag{3}$$

The drawbacks of the real discrete wavelet transform are: oscillations (since wavelets are band-pass functions, the wavelet coefficients tend to oscillate positive and negative around singularities), invariant translations (if the input signal is translate will produce different wavelet coefficients) and aliasing (when the wavelet coefficients are computed via iterated discrete-time down sampling operations combined with nonideal low-pass and high-pass filters). To overcome these limitations the complex wavelet transforms have been developed. They are defined by [2]:

$$\Psi_{c}(t)=\Psi_{r}(t)+j\Psi_{i}(t) \tag{4}$$

where $\Psi_{c}(t)$ is the complex wavelet transform, $\Psi_{r}(t)$ and $\Psi_{i}(t)$ are two real wavelet transforms, first of them is the real part and the second is the imaginary part of complex wavelet transform.

The real 2-D dual-tree wavelet transform is implemented using two parallel discrete wavelets. Hence six wavelets are associated to the real 2-D dual-tree wavelet transform. The complex 2-D dual-tree wavelet transform is implemented with two real 2-D dual-tree wavelet transform. In this case, twelve wavelets are associated to the complex 2-D dual-tree wavelet transform (six for the real part and six for the imaginary part). The two discrete wavelets use two sets of filters: (a_0, a_1) for higher filter zone and (b_0, b_1) for lower filter zone. The complex wavelet transform with dual tree CWT-DT is implemented by iteration of filters sets for sub-bands. The de-noising threshold T can be set so the frequency smaller that the threshold T are assigned to zero. The next step is to apply the inverse complex wavelet transform with dual tree to reconstruct the image.

2.2 Signal to noise ratio

The grayscale (atonal) MxN size images were analysed. The original image is denoted by the two-dimensional array f and the noised image is represented by the two-dimensional array g. Here M is the rows number or image height and N is the number of the columns or image width. We noted with f(i, j) and g(i, j) respectively, the grey

intensity level of the pixel at the intersection of row i and column j for f and g images. The f(i, j) and g(i, j) values are in the range 0 (black colour) to 255 (white colour).

To determine the quality of processed images the SNR, PSNR, MSE, and MAE quality parameters [7, 8] were used.

$$SNR = 10\log\frac{\sum_{i=0}^{N-1}\sum_{j=0}^{M-1} f^2(i,j)}{\sum_{i=0}^{N-1}\sum_{j=0}^{M-1}\left(g(i,j)-f(i,j)\right)^2}\,(\mathrm{dB}) \quad \text{(signal to noise ratio)} \tag{5}$$

$$\mathrm{PSNR} = 10\log\frac{\mathrm{N}\cdot\mathrm{M}\left(\max\limits_{i,j} f(i,j)\right)^2}{\sum_{i=0}^{N-1}\sum_{j=0}^{M-1}\left(g(i,j)-f(i,j)\right)^2}\,(\mathrm{dB}) \quad \text{(peak signal to noise ratio)} \tag{6}$$

$$\mathrm{MSE} = \frac{1}{\mathrm{N}\cdot\mathrm{M}}\sum_{i=0}^{N-1}\sum_{j=0}^{M-1}\left(g(i,j)-f(i,j)\right)^2 \text{ (mean squared error)} \tag{7}$$

$$\mathrm{MAE} = \frac{1}{\mathrm{N}\cdot\mathrm{M}}\sum_{i=0}^{N-1}\sum_{j=0}^{M-1}\left|g(i,j)-f(i,j)\right| \text{(mean absolute error)} \tag{8}$$

SNR is the ratio between energy of de-noised signal and the energy when of overlapped noise. PSNR has done the ratio between maximum energy of de-noised signal and the energy of overlapped noise. MSE quantifies the difference between estimated values and true values of the parameter. MAE is an average of the absolute difference between estimated values and true values.

3. RESULTS AND DISCUSSIONS

The ultrasound images were acquired using the scanning systems VIVID E9, GE HORTEN MOK WAY.

The Figures 1 (a) and (b) show examples of the original ultrasound images used in this study. The images represent the right side of myocardium (right atrium and ventricle) with tricuspid valve. The Figure 1 (a) corresponds to the atrial systole phase of the cardiac cycle and the Figure 1 (b) corresponds to the atrial diastole phase. The Figures 2 (a) and (b) show ultrasound images from Figures 1 (a) and (b) affected by additive Gaussian noise with amplitude of 10. The raw data were analysed in the *MATLAB* program. The image parameters are: bitmap images, size 512x512 pixels, 8 bit/pixel.

(a) (b)

Fig.1. Original images: (a) atrial diastole, (b) atrial systole.

(a) (b)

Fig. 2. Gaussian noise with amplitude of 10 added in images presented in Figure 1.

The Figures 3 (a-d) present examples of the image 2 (a) subsequent to de-noising operation when various threshold values have been used.

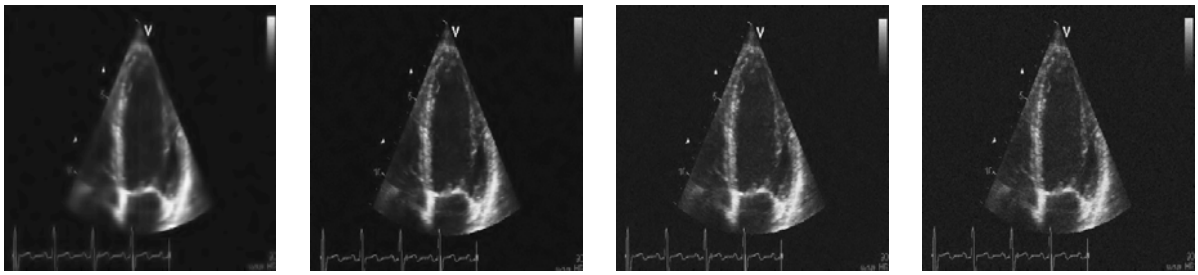

(a) T=40 (b) T=10 (c) T=5 (d) T=2

Fig. 3. Image 2 (a) de-noised using CWT-DT method using various T threshold values.

The Figures 4 (a-d) present the pixel of image 2 (a) affected by the de-noising technique (black zones) at the first iteration level of complex wavelet transform with dual-tree and for different threshold values.

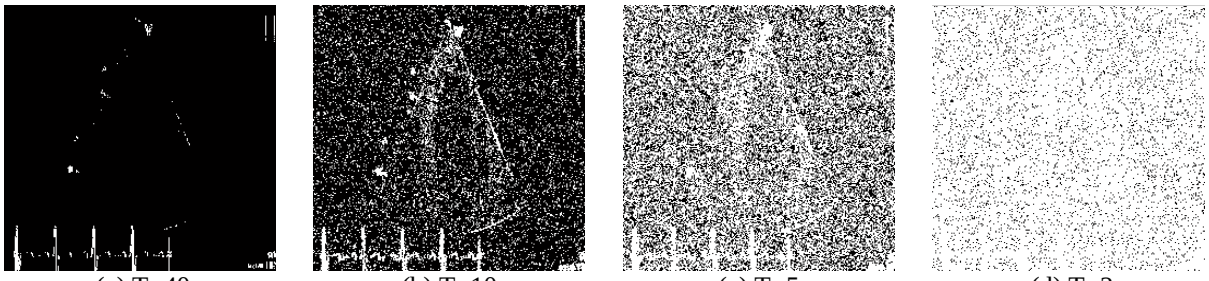

(a) T=40 (b) T=10 (c) T=5 (d) T=2

Fig. 4. Pixels of image 2 (a) affected by de-noise technique at first iteration of CWT-DT at various T threshold values.

Figure 5 present the resulting de-noised image using the median filter for Figure 1 (a):

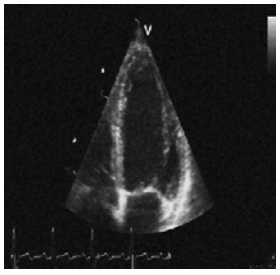

Fig. 5. Image 2 (a) de-noised with a median filter.

The results presented in Table 1 were used for comparison purposes.

Table 1. The measured quality parameters for de-noised images at various threshold values.

Method	Image	SNR	PSNR	MSE	MAE
CWT-DT, T=40	Fig. 2 (a)	12.24	76.61	77.32	3.56
	Fig. 2 (b)	11.87	76.60	77.63	3.54
CWT-DT, T=30	Fig. 2 (a)	13.61	77.98	56.43	3.15
	Fig. 2 (b)	13.25	77.98	56.46	3.12
CWT-DT, T=20	Fig. 2 (a)	15.65	80.02	32.25	2.62
	Fig. 2 (b)	15.26	79.99	35.54	2.61
CWT-DT, T=16	Fig. 2 (a)	16.83	81.20	26.90	2.36
	Fig. 2 (b)	16.45	81.17	27.05	2.36
CWT-DT, T=15	Fig. 2 (a)	17.15	81.52	24.97	2.32
	Fig. 2 (b)	16.75	81.48	25.23	2.32
CWT-DT ,T=14	Fig. 2 (a)	17.49	81.86	23.12	2.26
	Fig. 2 (b)	17.14	81.86	23.10	2.23
CWT-DT ,T=13	Fig. 2 (a)	17.79	82.16	21.56	2.24
	Fig. 2 (b)	17.47	82.19	21.39	2.22
CWT-DT, T=12	Fig. 2 (a)	18.17	82.54	19.74	2.21
	Fig. 2 (b)	17.85	82.58	19.58	2.20
CWT-DT, T=11	Fig. 2 (a)	18.54	82.91	18.15	2.21
	Fig. 2 (b)	18.11	82.84	18.44	2.22
CWT-DT ,T=10	Fig. 2 (a)	18.76	83.13	17.26	2.29
	Fig. 2 (b)	18.48	83.20	16.56	2.26
CWT-DT, T=9	Fig. 2 (a)	18.94	83.31	16.52	2.41
	Fig. 2 (b)	18.55	83.28	16.67	2.40
CWT-DT, T=8	Fig. 2 (a)	18.83	83.20	16.95	2.62
	Fig. 2 (b)	18.48	83.20	16.97	2.62
CWT-DT, T=7	Fig. 2 (a)	18.45	82.82	18.50	2.94
	Fig. 2 (b)	18.09	82.81	18.54	2.94
CWT-DT, T=6	Fig. 2 (a)	17.79	82.16	21.54	3.36
	Fig. 2 (b)	17.45	82.18	21.47	3.35
CWT-DT, T=5	Fig. 2 (a)	16.82	81.19	26.97	3.91
	Fig. 2 (b)	16.48	81.20	26.87	3.90
CWT-DT, T=4	Fig. 2 (a)	15.73	80.10	34.62	4.54
	Fig. 2 (b)	15.35	80.07	34.85	4.56
CWT-DT, T=3	Fig. 2 (a)	14.49	78.86	46.13	5.32
	Fig. 2 (b)	14.08	78.81	46.65	5.35
CWT-DT, T=2	Fig. 2 (a)	13.29	77.66	60.82	6.17
	Fig. 2 (b)	12.97	77.70	60.22	6.13
Median Filter	Fig. 2 (a)	11.12	27.75	7.98	100.04
	Fig. 2 (b)	10.79	27.77	7.97	99.57

The quality parameters of the de-noising image ultrasound image from Figure 2 (a) evolution versus the threshold values are given in Figure 6.

The complex wavelet transform with dual tree is a tool to establish the optimal threshold in order to obtain an optimal quality image. In this respect, the threshold T has been modified from lower values to higher values. A sound analysis of images (Figures. 2 (a-b) and Figures. 3 (a-d)) has been performed by a radiology specialist. Her analysis allows the following conclusions: at higher threshold value (T>15) the noise is removed, but image details are blurred. For a lower threshold (T<5) the noise is not totally removed. The principle of the thresholding method using complex wavelet transform with dual-tree permits the explanation of these findings. For a higher threshold value more detailed pixels belonging to high sub-band frequency are affected by setting to zero. So we removed the noised pixels, on one hand, and the detail pixels, on the other hand. For a lower threshold value, near to zero, the noise is not affected by threshold technique. The Figures 3 (d-a), confirm our ideas, namely when the threshold increases more pixels in the processed image with the CWT-DT are affected.

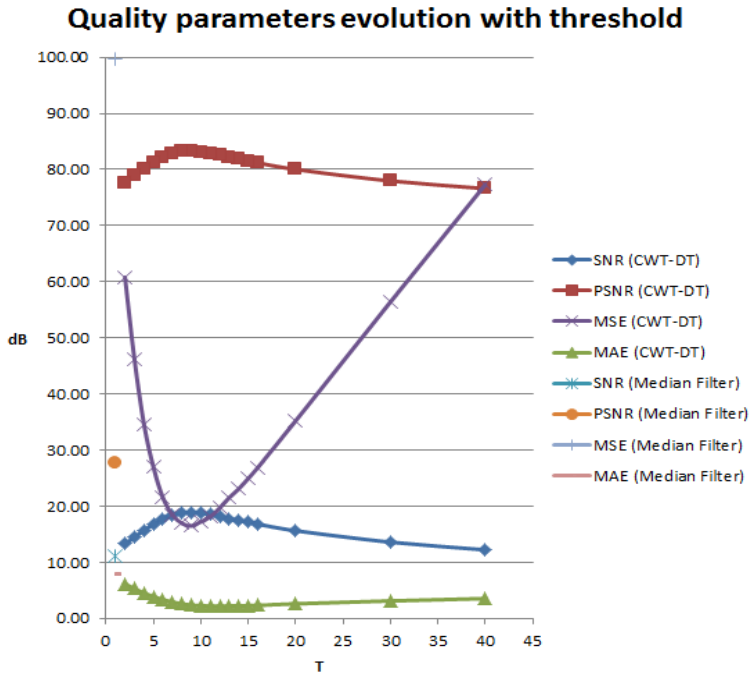

Fig. 6. Quality parameters evolution vs. threshold values.

This idea is confirmed by analysis of the quality parameters presented in table 1 and the data plotted in Figure 6. The SNR and PSNR parameters starting from lower threshold values increase to a maximum value (located at T=9 for the first analysed image and T=10 for the second analysed image) and then decrease. The MAE and MSE parameters decrease starting from lower threshold values to a minimum (located at T=10 (MSE), T=13 (MAE) for the first analysed image and T=9 (MSE), T=11 (MAE) for the second analysed image) and the increase. The lower values of the SNR and PSNR parameters and the higher values of the MAE and MSE parameters signify a small quality improvement between the noised image and the processed (de-noised) image. In this case, the result of the de-noising process is unsatisfactory. On the contrary, the higher values of the SNR and PSNR parameters and the lower values of the MAE and MSE parameters indicate a high quality of de-noising process. Therefore, the optimal threshold corresponding to CWT-DT de-noising operation must be sought between T=9, T=10, T=11, T= 13 values.

Based on the above presented analyse we proposed the [6, 15] range of the threshold values which assures accurate de-noising results in echocardiography images using the CWT-DT filtering technique. For T values less than 6, the noise is not completely removed. For T values higher than 15, the result of the de-noising process is a blurred image.

These results are compared with data provided by median filtering. According to radiology specialist the images obtained using the median filtering techniques (Figure 5) are affected by noise. Looking to the values of the quality parameters, the quality of the de-noised ultrasound images using the median filter (Table 1 or Figure 6) are similar to the CWT-DT filtering with T<2 threshold. This denotes the poor quality of the results obtained based on the median filtering technique and the superior quality of the results obtained using the CWT-DT filtering technique. In conclusion: (a) Median filter reduces the Gaussian noise. (b) By using wavelet filter, a considerable amount of speckle noise is removed, than the median filter. From the results presented in Table 1, it is observed that the proposed CWT-DT method outperforms the median methods in terms of SNR, PSNR, MSE, and MAE.

As a final remark, if the ratio of noise into echography image increases/decreases, then the optimal threshold value used to de-noise the cardiac ultrasound image applying complex wavelet transform with dual-tree increases/decreases proportionally.

4. CONCLUSIONS

We have presented a method based on complex wavelet transform with dual tree for de-noising ultrasound cardiac images. Our results and their interpretation allow us to conclude that the optimal threshold value for de-noising operation using the complex wavelet transform with dual-tree is located between 6 and 15. De-noising of ultrasound images with CWT-DT is more efficient than median filtering method. The results obtained are in accordance with physicians' opinion about the processed images. The method under discussion is very useful in improving the quality ultrasound images. In the future we intend to expand the database of cardiac cycle ultrasound images and to develop an algorithm for automatically ultrasound cardiac cycle images de-noising based on neuronal networks. Moreover, the present results represent a first step in our research plan of development of an automatic CADi system capable to accurately distinguish between the two cardiac cycle phases, atrial systole and atrial diastole.

ACKNOWLEDGMENTS

The authors would like to thank the Project TOP ACADEMIC - 107/1.5/S id 76822 and the Project SOP HRD-EFICIENT 61445/2009 of "Dunarea de Jos" University of Galati, Romania.

REFERENCES

[1] De Rivaz, P.F.C., Kingsbury, N.G., Complex wavelet features for fast texture image retrieval, IEEE International Conference on Image Processing, Vol.1, Issue 5, 1999, p.109-113.
[2] Selesnick, I.W., Baraniuk, R.G., Kingsbury, N.G., The dual-tree complex wavelet transform, Signal IEEE Signal Processing Magazine, Vol. 22, Issue 6, 2005, p. 123-151.
[3] Sathesh, Manoharan, S., A dual tree complex wavelet transform construction and its application to image denoising, International Journal of Image Processing, Volume 3, Issue 6, 2010, p. 293-300.
[4] Chang, S.G., Bin, Y., Vetterli, M., Adaptive wavelet thresholding for image denoising and compression, IEEE Transaction on image processing, Vol.9, No.9, 2000, p.1532 – 1546.
[5] Brannock, E., Weeks, M., Edge detection using wavelets, Proceedings of the 44th annual South-East regional conference ACM New York, NY, USA, 2006, p. 649-654.
[6] Daubechies, I., Ten lectures on wavelets, SIAM, 1992.
[7] Suryanarayana, S., Deekshatulu, B.L., Kishore, K.L., Kumar, R., Novel impulse detection technique for image denoising, Journal of Theoretical and Applied Information Technology, Vol.5, No.2, 2009, p. 102-106.
[8] Thangavel, K., Manavalan, R., Aroquiaraj, I.L., Removal of speckle noise from ultrasound medical image based on special filters: Comparative study, ICGST-GVIP Journal, Vol.9, Issue 3, 2009, p. 25-32.
[9] Gencay, R., Seluk, F., Whitcher, B., An Introduction to Wavelets and Other Filtering Methods in Finance and Economics, Academic Press, 2002.